Observational Strategies for Local Acoustic Source Detection with DKIST/VTF

C. Morrell [1, 2], M. P. Rast [1, 2], S. M. Bahauddin [1, 4], I. Milić [3]

[1]Laboratory for Atmospheric and Space Physics, University of Colorado, Boulder, CO

[2]Department of Astrophysical and Planetary Sciences, University of Colorado, Boulder, CO

[3]Institut für Sonnenphysik, Freiburg im Breisgau, Germany

[4]Center for Astronomy, Independent University Bangladesh, Dhaka, Bangladesh

Full Paper Text
NASA ADS Link

Motivation: Why Observe Local Acoustic Sources?

Solar acoustic oscillations (p-modes) are thought to be sustained by continuous stochastic excitation [1] resulting from turbulent convection. The primary physical mechanisms responsible for this excitation are:

- Mechanical driving via **Reynolds stresses** [2, 3, 4, 1] (i.e., Lighthill's acoustic analogy)
- Thermodynamic driving via **entropy fluctuations** caused by strong localized cooling [5, 6, 7] (e.g., granule fragmentation [8])

It is likely that each mechanism contributes to the solar p-mode spectrum, yet **several questions remain**:

- How are the sources **distributed with depth**?
- What is the temporal phasing between the **thermodynamic and dynamic fluctuations** associated with the sources?
- How efficiently does each mechanism **couple to the global modes**?

Observing individual acoustic excitation events directly may allow us to better constrain these questions.

Challenges: What Necessitates Direct Spectral Detection?

Traditional image filtering techniques are largely ineffective for local acoustic wavefront detection because the **locally generated wavefronts have amplitudes several orders of magnitude smaller than the background** (i.e., global p-modes and granular motions).

The novel detection method of [9, 10] leverages the difference between the evolution timescales of the wavefronts of interest and the background dynamics. **Using a temporal difference filter**, we can identify acoustic wavefronts propagating outward from local sources in MHD simulations. However, **challenges remain in detecting these waves in observations**.

In particular, preliminary analysis shows that inversions fail to recover these local wavefront signatures. **This motivates direct detection of the wavefront signatures within the observed spectrum.**

Aims of This Paper

1. **Which wavelengths are most sensitive** to temperature perturbations induced by local acoustic wavefronts?
2. Can we design a **DKIST/VTF observing strategy** that could make detecting these waves possible?

Methods: Wavefront Detection in MURaM

We use the temporal difference filter of [9, 10] to identify an acoustic wavefront propagating across a granule in the MURaM simulation [11].

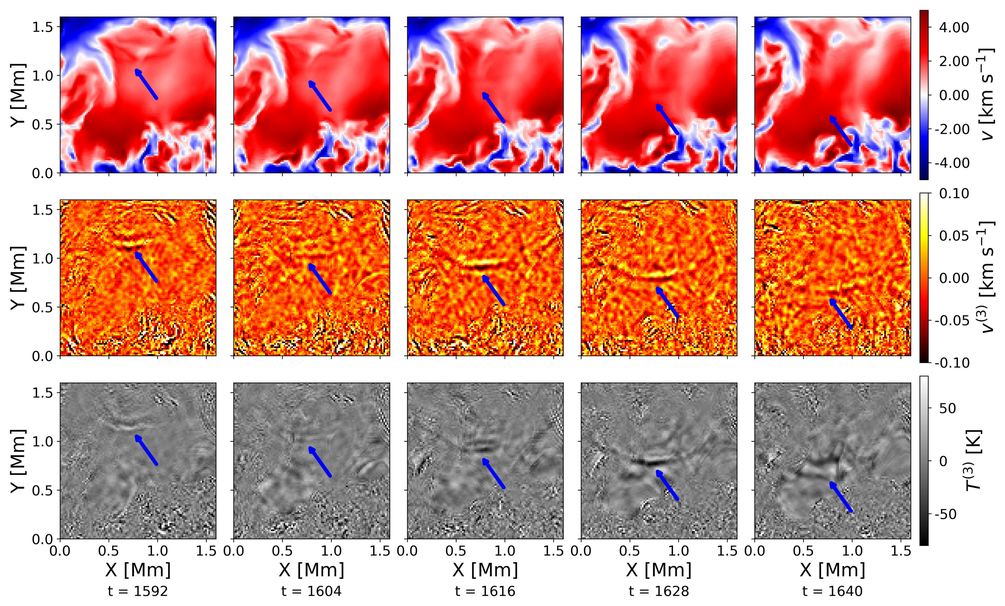

Figure 1. Propagation of a localized acoustic wavefront through the photosphere of the MURaM radiative MHD simulation. Panels show snapshots of LOS velocity (*top*), its third-order temporal difference (*middle*), and the corresponding third-order temporal difference in temperature (*bottom*), revealing a coherent wavefront expanding across a granule.

Methods: Spectral Synthesis and Response Function Analysis

We use the SNAPI code [12] to synthesize three photospheric lines (Fe I 5250.2, Fe I 5250.6, and Fe I 6302.5) under the assumption of LTE. We treat each pixel in the MURaM wavefront as a 1D atmosphere and use these as inputs for the synthesis. Using SNAPI, we also calculate the **temperature response functions**.

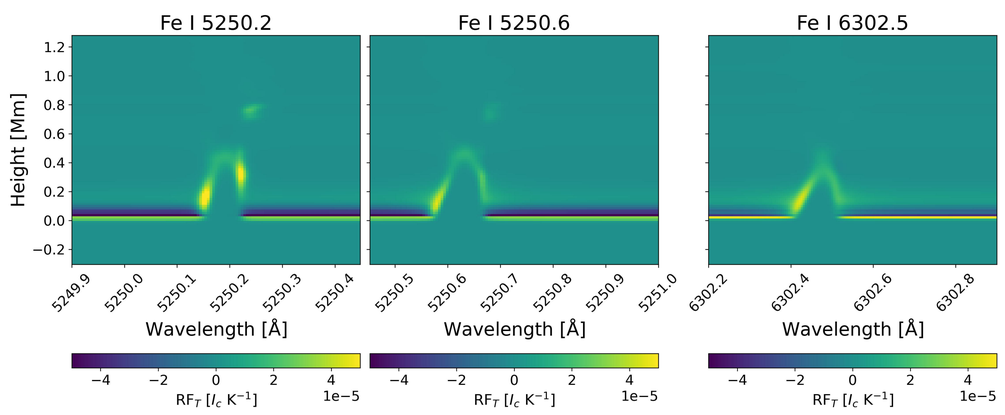

Figure 2. Temperature response functions for three photospheric Fe lines generated using SNAPI [12].

Methods: The Sensitivity Measure

To determine which wavelengths are most sensitive to temperature perturbations induced by local acoustic wavefronts, we use the response function to define a **wavelength-dependent sensitivity measure** $\mathcal{S}(\lambda, t)$ as the ratio of the expected intensity change due to wave-induced temperature perturbations to the expected intensity change due to other temperature fluctuations (i.e., granulation).

Key Result: Wavefront Signatures in the Blue Wing of Photospheric Lines

The **asymmetric response** causes the blue wing of each line to be **less steep**. This **restricts the range of heights** which contribute to the observed intensity changes caused by temperature perturbations. This is ideal for **isolating the faint signature of the wavefront**.

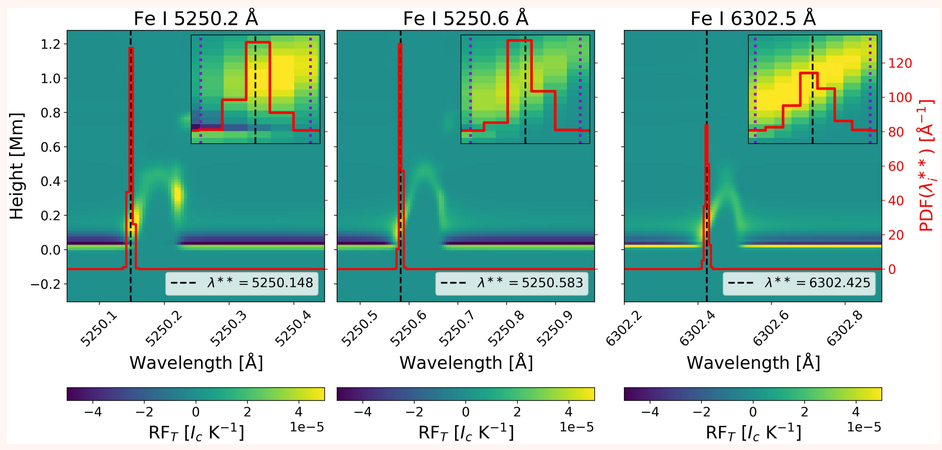

Figure 3. The PDF of the wavelength at which $\mathcal{S}(\lambda, t)$ is highest at any time (λ^{**}) for each pixel in the wavefront (*solid red line*) overplotted on the temperature response functions. The insets zoom into the λ^{**} region and indicate the extent of the VTF spectral element (*dotted vertical lines*).

Key Result: Temporal Shift of Ideal Wavelength Towards Line Center

The sensitivity of synthetic Stokes I to temperature perturbations shifts to higher atmospheric layers as the acoustic wavefront propagates upward. Thus, the temporal evolution of the wavelength of maximum sensitivity $\lambda^*(t)$ towards line center **traces the upward propagation of the wavefront**.

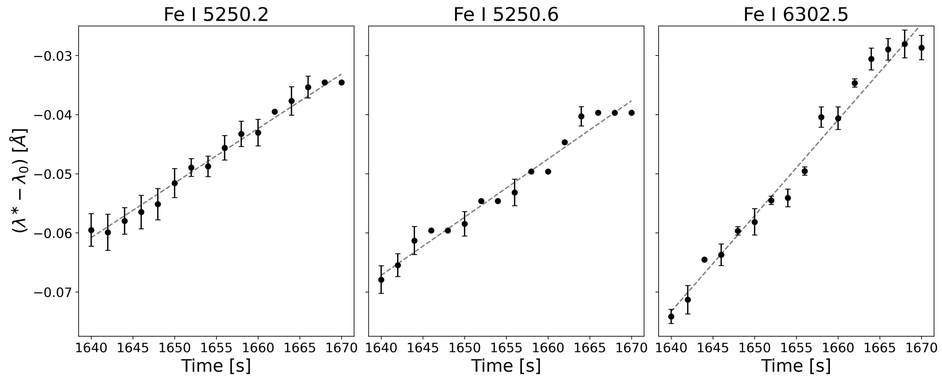

Figure 4. Time-dependent drift of the wavelength of maximum temperature sensitivity, $\lambda^*(t)$. Error bars indicate the standard deviation of λ^* over pixels.

Implications for DKIST/VTF

Observing Strategy I: Monochromatic

- Critical sampling of the wavefront occurs at **1 s cadence**
- We suggest **monochromatic sampling at λ^{**}** with a cadence of 0.5 s
- This **over-samples** the expected wavefront propagation while maintaining a high SNR (≈ 817)

Observing Strategy II: Multi-Wavelength

- We suggest observing **the blue wing of Fe I 6302.5** (due to the shallow slope) and **interleaving observations over three wavelengths**, λ^{**} and $\lambda^{**} \pm 0.0315$, with 0.48 s cadence
- **Post-observational analysis** should focus on shifting the data accumulated at different wavelengths and times so that they can be added together to reinforce the wavefront signal

References

[1] P. Goldreich and D. A. Keeley. Solar seismology. II. The stochastic excitation of the solar p-modes by turbulent convection. , 212:243–251, February 1977.

[2] M. J. Lighthill. On Sound Generated Aerodynamically. I. General Theory. *Proceedings of the Royal Society of London Series A*, 211(1107):564–587, March 1952.

[3] M. J. Lighthill. On Sound Generated Aerodynamically. II. Turbulence as a Source of Sound. *Proceedings of the Royal Society of London Series A*, 222(1148):1–32, February 1954.

[4] R. F. Stein. Generation of Acoustic and Gravity Waves by Turbulence in an Isothermal Stratified Atmosphere. , 2(4):385–432, December 1967.

[5] R. F. Stein and Å. Nordlund. Convection and Its Influence on Oscillations. In Douglas Gough and Juri Toomre, editors, *Challenges to Theories of the Structure of Moderate-Mass Stars*, volume 388, page 195, 1991.

[6] P. Goldreich, Norman Murray, and P. Kumar. Excitation of Solar p-Modes. , 424:466, March 1994.

[7] M. P. Rast. Photospheric Downflows: How deep, how coherent, how important? In F. P. Pijpers, J. Christensen-Dalsgaard, and C. S. Rosenthal, editors, *SCORe'96 : Solar Convection and Oscillations and their Relationship*, volume 225, pages 135–138, 1997.

[8] M. P. Rast. On the Nature of "Exploding" Granules and Granule Fragmentation. , 443:863, April 1995.

[9] S. M. Bahauddin and M. P. Rast. Identifying Acoustic Wave Sources on the Sun. I. Two-dimensional Waves in a Simulated Photosphere. , 915(1):36, July 2021.

[10] S. M. Bahauddin and M. P. Rast. Identifying Acoustic Wave Sources on the Sun. II. Improved Filter Techniques for Source Wavefield Seismology. , 955(1):31, September 2023.

[11] M. Rempel. Numerical Simulations of Quiet Sun Magnetism: On the Contribution from a Small-scale Dynamo. , 789(2):132, July 2014.

[12] I. Milić and M. van Noort. Spectropolarimetric NLTE inversion code SNAPI. , 617:A24, September 2018.